

УДК 544.163.2 : 544.228

V.S. Urusov, E.V. Leonenko

Lomonosov Moscow State University
1, Vorobievy Gory, GSP-1, 119992, Moscow, Russia
E-mail: urusov@geol.msu.ru; egorleo@mail.ru

ATOMISTIC COMPUTER SIMULATION OF ABO_3 , (A = Ca; B = Zr, Ti, Sn) PEROVSKITES: CRYSTAL STRUCTURE, INTRINSIC POINT DEFECTS AND DOPANT FORMATION

The modeling of structural and thermodynamic properties of *complex* oxides with *orthorhombic* perovskite structure CaZrO_3 , CaTiO_3 and CaSnO_3 was performed by means of atomistic computer pair potentials method in ionic approximation. The results of calculations for the structural properties are in a good agreement with experimental data and previous calculations, while the calculated values of bulk modules are overestimated. The calculated entropy values for the room temperature are in a good agreement with available experimental data for CaTiO_3 and CaZrO_3 . For the first time the entropy was calculated in the temperature range 300–1800 K for all three perovskites and the results are in a satisfactory agreement with experimental data for CaTiO_3 . The formation energies of isolated intrinsic point defects in these crystals were calculated by using Mott-Littleton approximation. For all three perovskite structures the most energetically favorable appears to be a Ca—O Schottky defect. The solution energies of the isovalent tetravalent substitutions (Zr^{4+} , Ti^{4+} , Sn^{4+} , Hf^{4+} , U^{4+} , Th^{4+}) in CaZrO_3 , CaTiO_3 , CaSnO_3 were also found in the approximation of infinite dilution. The enthalpies of mixing of the continuous binary solid solutions $\text{CaZrO}_3 - \text{CaTiO}_3$, $\text{CaTiO}_3 - \text{CaSnO}_3$, $\text{CaSnO}_3 - \text{CaZrO}_3$ were obtained by using of simple mixture model. The solution of the isolated trivalent dopants (Sc^{3+} , Y^{3+} , Cr^{3+} , Fe^{3+} , La^{3+}) and the tetravalent (Hf^{4+} , U^{4+} , Th^{4+}) dopants were considered both in A and B (A = Ca, B = Zr, Ti, Sn) sites of all three perovskites. According to these calculations, the most energetically favorable mechanism of incorporation of the trivalent dopants is the self-compensation at simultaneous substitutions on A and B sites. The most favorable way of incorporation of the tetravalent ions M^{4+} is an isovalent substitution of B^{4+} ion.

1. Introduction

1.1. *The aim of present study.* The new mineral lakargite [8] from perovskite family belongs to the ternary solid solution $\text{CaZrO}_3 - \text{CaTiO}_3 - \text{CaSnO}_3$ with a maximum CaZrO_3 content of 93 mole %, maximum CaTiO_3 content of 22 mole %, and maximum CaSnO_3 content of 20 mole %. Besides these three main components, the significant impurities in lakargite are Sc, Cr, Fe, Ce, La, Hf, Nb, U, and Th. The main component of solid solution CaZrO_3 has a broad range of applications, from proton conductors to ceramics used for immobilization of long-lived radionuclides. Perovskite CaTiO_3 is widely used in electronics as a ceramic dielectric material and in immobilization of radioactive waste. CaSnO_3 is a potentially important material for application as a capacitor com-

ponent. The solid solutions of these materials are attractive candidates for use in many electronic applications. The structure of $\text{CaZr}_{1-x}\text{Ti}_x\text{O}_3$ solid solution was studied earlier [11, 14], $\text{CaZr}_{1-x} \times \text{Sn}_x\text{O}_3$ and $\text{CaSn}_{1-x}\text{Ti}_x\text{O}_3$ solid solutions are not so well examined. The electronic properties of perovskite materials and their solid solutions depend on type and concentration of point defects in them. The aim of this work is a study of the defect structure of pure and doped materials CaZrO_3 , CaTiO_3 , CaSnO_3 by means of computer modeling. Calculations of structure, properties and formation energy of intrinsic point defects and isolated dopants in CaZrO_3 , CaTiO_3 , CaSnO_3 were performed by means of an atomistic pair potentials method. On the basis of the obtained data the mixing enthalpies of the binary solid solutions $\text{CaZrO}_3 - \text{CaTiO}_3$, $\text{CaTiO}_3 - \text{CaSnO}_3$, $\text{CaSnO}_3 - \text{CaZrO}_3$ were estimated with the help of a subregular mixing model.

1.2. Crystallography of orthorhombic perovskites. The ideal oxide perovskite structure ABO_3 consists of small B cations within the oxygen octahedra and large A cations which are 12-fold coordinated by oxygen. The ideal atomic packing of the perovskite lattice results in a cubic structure with space group $Pm3m$, but as the ionic radii of the A and B cations move away from the values that give a tolerance factor $\tau = 1.0$ the BO_6 octahedra tilt to yield lower symmetry arrangements.

All materials considered here (CaTiO_3 , CaSnO_3 and CaZrO_3) display a distorted orthorhombic structure with the space group $Pnma$. The structure of perovskite CaTiO_3 is less distorted ($\tau = 0.97$), than CaSnO_3 ($\tau = 0.93$) and CaZrO_3 ($\tau = 0.92$) [26]. This sequence is in agreement with the range of octahedral ionic radii of Ti^{4+} , Sn^{4+} and Zr^{4+} (0.61, 0.69 and 0.72 Å, respectively).

2. Methodology and interatomic potentials

The calculations presented here are based on a classical description of an ionic crystal lattice. The forces acting between ions consist of two main terms: long-range coulombic, which are summed via the Ewald method, and short-range pair terms, which are modeled using Buckingham type potentials [2]. The lattice energy can be expressed as follows:

$$V_{ij}(R_{ij}) = \sum_{j>i} \sum_i Z_i Z_j / R_{ij} + \lambda_{ij} \exp(-R_{ij} / \rho_{ij}) - C_{ij} / R_{ij}^6, \quad (1)$$

where λ_{ij} , ρ_{ij} and C_{ij} are short-range adjustable parameters, R_{ij} is the distance between i - and j -ions and Z_i , Z_j are the formal charges on ions i and j ,

Table 1. Parameters of short-range Buckingham potentials for CaZrO_3 , CaTiO_3 and CaSnO_3

Interaction	λ , eV	ρ , Å	C , eV·Å ⁶
$\text{Ca}^{2+}-\text{O}^{2-}$	1340.18	0.321	0.0
$\text{Zr}^{4+}-\text{O}^{2-}$	1150.869	0.3750	0.0
$\text{Ti}^{4+}-\text{O}^{2-}$	840.2	0.3810	0.0
$\text{Sn}^{4+}-\text{O}^{2-}$	1285.2	0.3611	0.0
$\text{O}^{2-}-\text{O}^{2-}$	22764.0	0.1490	43.0

Species	$W(e)$	$Y(e)$	k , eV/Å ²
<i>Shell model parameters</i>			
Ca^{2+}	+3.135	-1.135	110.2
Zr^{4+}	+4.05	-0.05	160.6
Ti^{4+}	+1.11	+2.89	140.0
Sn^{4+}	+0.01	+3.99	220.0
O^{2-}	-2.077	+0.077	65.3

respectively. The parameters of the short-range potentials for pair atomic interactions were taken first from the database of interatomic potential parameters [15] and previous simulation studies of CaZrO_3 [5], and after that were optimized to fit the structural properties of the investigated crystals (Table 1). An agreement with the experimental data for these properties is rather good (Table 2).

The electronic polarizability of ions is included via the shell model developed by Dick and Overhauser [6, 18] and is an empirical means of coupling the electronic polarization to the ionic distortion in a given structural environment. This model describes such effects by treating each ion i in terms of a core with an effective charge W_i con-

Table 2. Unit cell volume V and parameters a , b , c , static dielectric constant $\langle \epsilon_s \rangle$ and dynamic dielectric constant $\langle \epsilon_\infty \rangle$, bulk modulus K , lattice energy E and standard entropy S_{300} of the investigated perovskites

CaTiO_3	Experimental data [3, 20]	This calculation	Calculation [17]
V , Å ³	223.682	224.754	226.3
a , Å	5.388	5.385	5.411
b , Å	5.447	5.440	5.439
c , Å	7.654	7.672	7.689
$\langle \epsilon_s \rangle$	180	17.6	—
$\langle \epsilon_\infty \rangle$	—	1.25	—
K , GPa	171(1)	215	—
E , kJ/mole	—	-14586.22	—
S_{300} , J/mole·K	93.64	94.34	—

CaSnO_3	Experimental data [20, 25]	This calculation
V , Å ³	248.4642	248.6584
a , Å	5.5320	5.5398
b , Å	5.6810	5.6406
c , Å	7.9060	7.9575
$\langle \epsilon_s \rangle$	—	21.1
$\langle \epsilon_\infty \rangle$	—	2.17
K , GPa	163(1)	198
E , kJ/mole	—	-14240.69
S_{300} , J/mole·K	—	95.02

CaZrO_3	Experimental data [10, 20]	This calculation	Calculation [5]
V , Å ³	258.265	258.269	253.678
a , Å	5.5912	5.6011	5.608
b , Å	5.7616	5.7085	5.665
c , Å	8.0171	8.0775	7.985
$\langle \epsilon_s \rangle$	—	73.1	16.39
$\langle \epsilon_\infty \rangle$	—	1.81	2.54
K , GPa	154(1)	184	—
E , kJ/mole	—	-13981.11	—
S_{300} , J/mole·K	96.4	96.3	—

nected via a harmonic spring to a massless shell with charge Y_i , so that the sum $W_i + Y_i = Z_i$. The harmonic spring constant k describes a rigidity of a connection between core and shell:

$$V_{sh} = (k/2)r^2, \quad (2)$$

where r is the distance between the centers of outer electronic shell and the core of the atom. The core and shell charges were taken from the databases of interatomic potential parameters [15, 18], and the constants k were altered to achieve as good as possible agreement of the calculated entropy at room temperature S_{300} of these materials with experimental data (Tables 1 and 2). All calculations of structural and thermodynamic properties were performed for orthorhombic unit cell consisting of 20 atoms ($Z = 4$).

Modeling of charged lattice defects was performed using the two-region Mott-Littleton approach [19], which divides the crystal lattice into two spherical regions, I and IIa, b. Ions in the central inner region I are relaxed explicitly using a Newton-Raphson procedure subject to the forces described by the interatomic potentials. Region IIa is an interfacial region in which the ions are relaxed in a single step, while the interaction energies between the ions in the region IIa and the region I are calculated explicitly. The outer region IIb is effectively a point charge array that provides the Madelung field of the remaining crystal. The region I was taken with a radius of 6.4 Å consisting of 162 ions, and the region IIa of radius 16.2 Å involved 2652 ions into calculation.

All calculations were carried out by means of the GULP program [7].

3. Results

3.1. Structural, elastic and thermodynamic properties. The structural properties (unit cell parameters a , b , c and volume V) of CaTiO_3 , CaSnO_3 and CaZrO_3 were equilibrated under the constant pressure conditions. The mean differences between the observed [3, 10, 25] and calculated lattice parameters are about $\pm 0.5\%$ (Table 2).

The calculated bulk moduli K of these crystals are higher than those observed experimentally [20]; the mean discrepancy is 19 %. This fact can be explained, as usual, by the relative rigidity of a theoretical crystal lattice in the purely ionic model.

The entropies S_T of the perovskites under investigation were calculated on the basis of the phonon spectra by means of GULP program in the temperature interval 300–1500 K. An average difference between calculated and available ob-

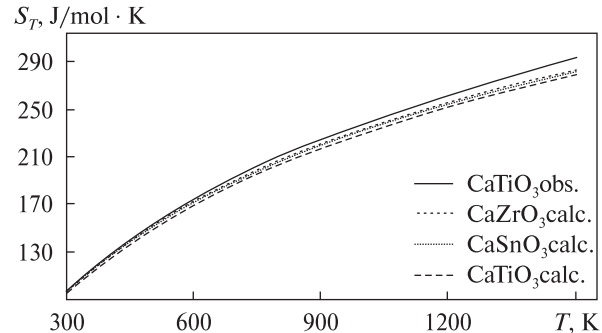


Fig. 1. Temperature dependences of entropies S_T of CaTiO_3 , CaSnO_3 and CaZrO_3

served data is 0.3 % at 300 K (Table 1). The discrepancy increases with temperature (Fig. 1), nevertheless, the maximal difference of the calculated and observed values for CaTiO_3 is 5.9 % at $T = 1500$ K. Recently [27] it was established by means of the high-temperature neutron diffraction method that at 1512 ± 13 K the orthorhombic $Pnma$ — tetragonal $I4/mcm$ reversible phase transition and at 1635 ± 2 K the tetragonal $I4/mcm$ — cubic $Pm3m$ transformation happen in this perovskite.

3.2. Intrinsic atomic defects. The energies of isolated point defects (vacancies and interstitials) were calculated by the Mott-Littleton approach using the potentials listed in Table 1. To calculate the energy of a vacancy, an ion was removed from its lattice site and placed at infinite distance. An interstitial ion was modeled in the same way by taking an ion from infinity and placing it on an interstitial site. The isolated defect energies were then combined to give the energies of formation of Frenkel and Schottky-type defects (Appendix). The lattice energies used in the calculation of Schottky type defects were obtained from the atomistic simulations of oxides in ionic approximation for TiO_2 [1, 17, 28] and SnO_2 [13], ZrO_2 [9], and from the Born-Haber cycle for CaO [16].

Examination of Appendix reveals that creation of Frenkel defects is associated with substantial amounts of energy, confirming that the dense perovskite structure is highly unlikely to accommodate ion interstitials. According to these calculations, for all of these materials Schottky defects are more likely to form, and for all three perovskite structures the most energetically favorable is $\text{Ca}-\text{O}$ Schottky defect. The calculated values are in a good correlation with previous atomistic calculations of a cubic modification of CaZrO_3 [4].

3.3. Evaluation of the mixing enthalpies in the case of isovalent substitutions. The energies of for-

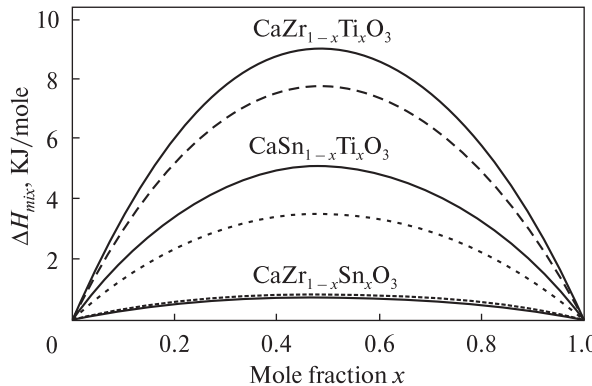
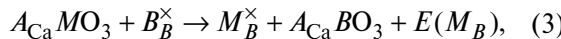


Fig. 2. Mixing enthalpies of solid solutions $\text{CaZr}_{1-x}\text{Ti}_x\text{O}_3$, $\text{CaSn}_{1-x}\text{Ti}_x\text{O}_3$, $\text{CaZr}_{1-x}\text{Sn}_x\text{O}_3$. Solid lines represent atomistic modeling, dashed lines represent the phenomenological model

mation of tetravalent isolated dopant defects M^{4+} ($M = \text{Zr}^{4+}, \text{Ti}^{4+}, \text{Sn}^{4+}$) on the octahedral B -site of the investigated perovskite materials $AB\text{O}_3$, i. e. incorporation of Sn and Ti into CaZrO_3 , and Sn and Zr into CaTiO_3 , and Ti and Zr into CaSnO_3 , were calculated using the Mott-Littleton approach (Table 3). The incorporation can be described by the following quasi-chemical reaction in Kröger-Vink notations:



where B_B^{\times} denotes a host metal ion on its own site, M_B^{\times} — a neutral dopant defect on B site, $E(M_B)$ is the energy of isovalent substitution $B^{4+} \rightarrow M^{4+}$.

On the basis of these data the energies of infinite dilution of the isovalent impurities Q (Margules parameters) were calculated by the following equation:

$$Q_X = E(M_B) + U_{AB\text{O}_3} - U_{AMO_3}, \quad (4)$$

where $U_{AB\text{O}_3}$ and U_{AMO_3} are the lattice energies of the corresponding crystals. The Margules parameters were used in evaluation of the mixing enthalpies of the $\text{CaZr}_{1-x}\text{Ti}_x\text{O}_3$, $\text{CaZr}_{1-x}\text{Sn}_x\text{O}_3$ and

Table 3. Energy of formation of the dopant defects and calculation of the Margules parameters, eV

Property		CaZrO_3	CaTiO_3	CaSnO_3
Lattice energy U		-144.904	-151.176	-147.595
Solution energies E	Zr^{4+}	—	6.668	2.720
	Ti^{4+}	-5.928	—	-3.372
	Sn^{4+}	-2.660	3.791	—
Margules parameters Q	Zr^{4+}	—	0.397	0.030
	Ti^{4+}	0.343	—	0.209
	Sn^{4+}	0.031	0.210	—

$\text{CaSn}_{1-x}\text{Ti}_x\text{O}_3$ solid solutions using the model of a subregular mixture:

$$\Delta H = x_1 x_2 (x_2 Q_1 + x_1 Q_2), \quad (5)$$

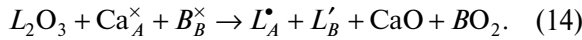
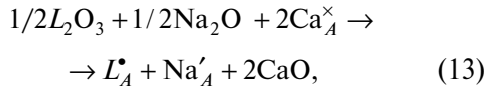
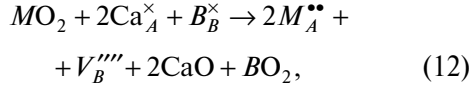
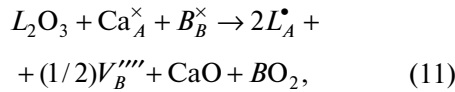
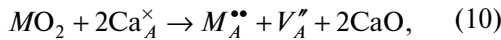
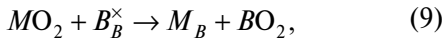
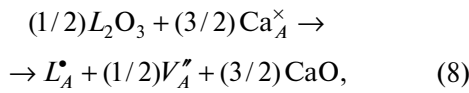
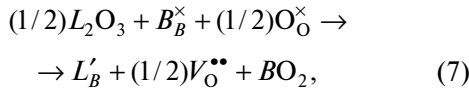
where x_1 and x_2 are the molar fractions of the components of the solid solutions, Q_1 and Q_2 are the corresponding Margules parameters for the end-members of the solid solution. The results are shown in the Fig. 2. The values of the mixing enthalpies were compared with those calculated in the framework of phenomenological model based on the crystal-chemical principles with regard to the lattice relaxation [22–24] by equation:

$$\Delta U_{\tilde{n}i} = (1/4)x_1 x_2 V K \delta_V^2, \quad (6)$$

where V and K are the molar volume and bulk modulus, the average value of the product $VK = 5930(110)$ kJ/mole without regard to compositions of all three solid solutions, δ_V is a volume mismatch parameter: $\Delta V/V(x) = (V_1 - V_2)/V(x)$, where $V(x) = x_1 V_1 + x_2 V_2$ is molar volume of a solid solution by using Retgers' volume additivity rule. Fig. 2 shows rather good agreement of the results of atomistic modeling with calculations based on the phenomenological model. This data allow us to estimate approximately a stability of the considered solid solutions [22–24]. Thus, the estimated critical temperature of decomposition T_{cr} for $\text{CaZrO}_3 - \text{CaTiO}_3$ system could be no more than 1850 K (without considering such additional factors as vibrational entropy), for $\text{CaSnO}_3 - \text{CaTiO}_3$ system $T_{cr} < 850$ K and for $\text{CaZrO}_3 - \text{CaSnO}_3$ system $T_{cr} < 200$ K. This means that only the last system forms continuous solid solutions at all temperatures above room temperature, two others can decompose at elevated temperatures. However, the mutual solubility limits can be sufficiently expanded in the ternary or more complicated system to which the mineral lakargiite [8] in fact belongs.

3.4. Incorporation of aliovalent dopant elements. Incorporation of the aliovalent cations on the A and B sites ($A = \text{Ca}$, $B = \text{Zr}, \text{Ti}, \text{Sn}$) of the perovskite crystals requires charge compensation by another lattice defect. The trivalent dopants L^{3+} ($\text{Sc}^{3+}, \text{Y}^{3+}, \text{Cr}^{3+}, \text{Fe}^{3+}, \text{La}^{3+}$) and tetravalent dopants M^{4+} ($\text{Hf}^{4+}, \text{U}^{4+}, \text{Th}^{4+}$) enter in the $AB\text{O}_3$ perovskite by the process of the substitution at either A^{2+} or B^{4+} positions. The compensation of an excess negative charge on the B -site substituted by L^{3+} ion is accomplished by formation of half the amount of oxygen vacancies V_O'' (see equation 7 below). In the case of formation of the excess

positive charge on A -site the compensations by cationic V_A'' (8, 10) and V_B''' (11, 12) vacancies should be taken into account in appropriate proportions. The tetravalent impurities incorporate into the B positions without any charge compensation (2 and 9). Simultaneous incorporation of Na^+ and the trivalent ion on the A -sites (13) and a self-compensation mechanism for trivalent ions (14) were also considered. These processes are described in the conventional Kröger-Vink notations (see Appendix) by the following reactions:



The energies of these reactions were evaluated by combining the appropriate defect and lattice energy terms. Such an approach provides useful systematic guide to the relative energies for different dopant species on the same site. For the calculations the pair ionic potentials of simple oxides from [15] were used and the defect energies were calculated by the Mott-Littleton approach. The lattice energies of oxides were calculated by the atomistic method, besides Na_2O , which lattice energy was calculated from Born-Haber cycle [16]. The resulting solution energies are presented in Table 4.

On Fig. 3 the dopant solution energies are presented as linear functions of the squared size mismatch parameter δ_R^2 calculated by the following equation [22–24]:

$$\delta_R^2 = (\Delta R / R)^2 = \left(\frac{r_h - r_d}{R} \right)^2, \quad (15)$$

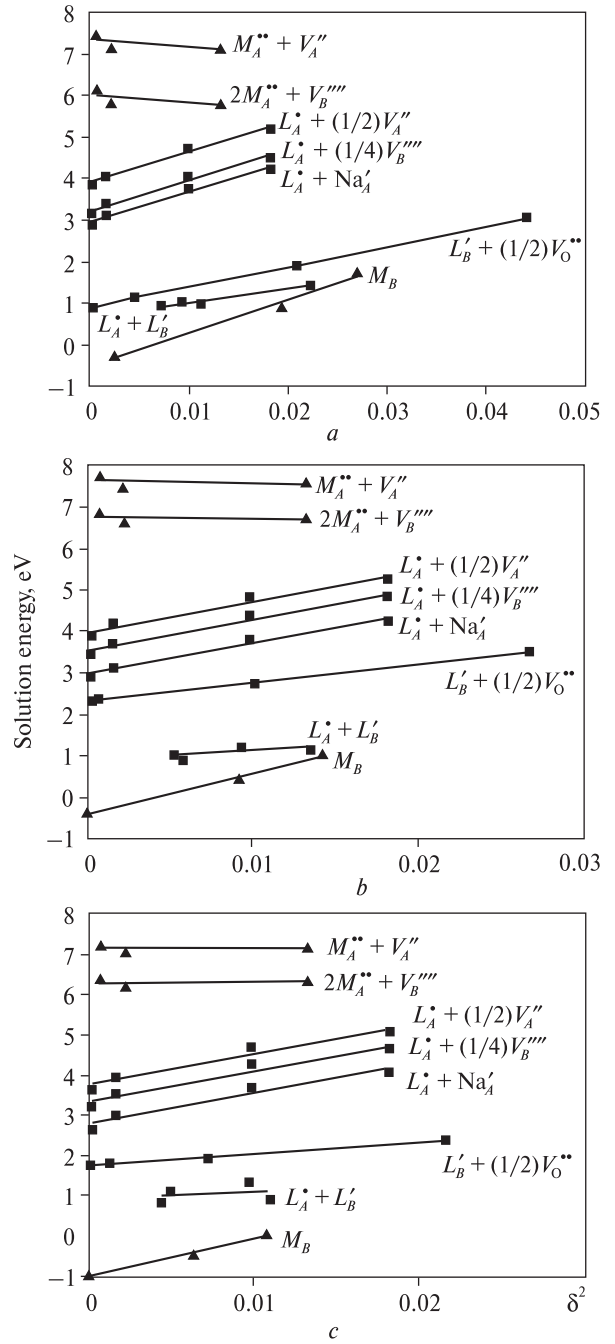


Fig. 3. Trivalent (squares) and tetravalent (triangles) dopant solution energies for $CaTiO_3$ (a), $CaSnO_3$ (b) and $CaZrO_3$ (c) host lattices as a function of size mismatch parameter δ^2

where r_h is a radius of a cation in the host lattice (B^{4+} and Ca^{2+}), r_d is a dopant ionic radius, R is a mean distance between host ion and oxygen, i. e. sum of their ionic radii. The values of ionic radii were taken from [21], in the case of incorporation into B position the dopant ionic radii correspond to 6-fold coordination, and into A position — to 8-fold coordination.

Table 4. Dopant solution energies for CaSnO_3 , CaTiO_3 , CaZrO_3 , eV

	$L'_B + (1/2) V_O^{''}$	$L_A^* + (1/2) V_A^{''}$	$L_A^* + (1/4) V_B^{''''}$	$L_A^* + L'_B$	$L_A^* + \text{Na}'_A$
CaSnO_3					
Sc ³⁺	1.50	4.55	4.05	0.43	3.51
Y ³⁺	1.99	4.07	3.57	0.44	3.03
Cr ³⁺	1.46	5.08	4.57	0.68	4.04
Fe ³⁺	1.38	4.91	4.40	0.55	3.86
La ³⁺	2.79	3.97	3.47	0.79	2.93
	M_B	$M_A^{''} + V_A^{''}$	$2M_A^{''} + V_B^{''''}$		
Hf ⁴⁺	-1.92	7.14	6.13	—	—
U ⁴⁺	-1.03	7.45	6.44	—	—
Th ⁴⁺	-0.39	7.72	6.71	—	—
	$L'_B + (1/2) V_O^{''}$	$L_A^* + (1/2) V_A^{''}$	$L_A^* + (1/4) V_B^{''''}$	$L_A^* + L'_B$	$L_A^* + \text{Na}'_A$
CaTiO_3					
Sc ³⁺	3.67	4.53	3.84	1.89	3.53
Y ³⁺	1.45	4.10	3.41	0.57	3.10
Cr ³⁺	0.06	5.02	4.33	0.33	4.02
Fe ³⁺	0.05	4.91	4.22	0.27	3.91
La ³⁺	2.78	4.07	3.39	1.22	3.07
	M_B	$M_A^{''} + V_A^{''}$	$2M_A^{''} + V_B^{''''}$		
Hf ⁴⁺	-1.84	7.04	5.67	—	—
U ⁴⁺	-0.38	7.59	6.21	—	—
Th ⁴⁺	0.45	7.85	6.47	—	—
	$L'_B + (1/2) V_O^{''}$	$L_A^* + (1/2) V_A^{''}$	$L_A^* + (1/4) V_B^{''''}$	$L_A^* + L'_B$	$L_A^* + \text{Na}'_A$
CaZrO_3					
Sc ³⁺	0.79	4.13	3.90	0.48	3.31
Y ³⁺	0.80	3.65	3.43	0.24	2.84
Cr ³⁺	0.89	4.57	4.35	0.75	3.76
Fe ³⁺	0.77	4.39	4.16	0.60	3.57
La ³⁺	1.56	3.43	3.20	0.51	2.61
	M_B	$M_A^{''} + V_A^{''}$	$2M_A^{''} + V_B^{''''}$		
Hf ⁴⁺	-2.46	6.03	5.57	—	—
U ⁴⁺	-1.81	6.22	5.77	—	—
Th ⁴⁺	-1.26	6.47	6.02	—	—

4. Discussion and conclusions

Examination of the results reveals several key points. The ionic model used in present work reproduces the structural properties of CaTiO_3 , CaSnO_3 and CaZrO_3 well. Nevertheless, the calculated bulk moduli of these crystals are higher than the observed ones. This fact can be explained by rigidity of the interatomic potentials in the ionic model. The good agreement of calculated entropies of the investigated perovskites with available experimental data has been achieved by em-

ployment of the shell model for all types of ions in the host lattice. This result displays that such a model can be used in further calculation of thermodynamic properties of solid solutions of these components.

The calculated properties of pure crystals are quite similar to the results of recent theoretical investigations for CaTiO_3 [1, 17] and CaZrO_3 [5]. The convergence of the calculated cell volumes of CaTiO_3 and CaZrO_3 with experimental data is better than for previous investigations [1, 5]. However,

APPENDIX

Energies of Frenkel and Schottky defects (eV/defect)

Defect notation		CaSnO_3	CaTiO_3	CaZrO_3	Calculation [4]
A , Frenkel	$\text{Ca}_A^X \rightarrow V_A^{''} + \text{Ca}_i^{''''}$	4.84	4.98	4.04	4.21
B , Frenkel	$B_B^X \rightarrow V_B^{''''} + B_i^{''''''}$	11.31	13.02	12.35	9.10
O, Frenkel	$\text{O}_O^X \rightarrow V_O^{''''} + O_i^{''''''}$	4.31	4.34	4.15	2.63
Full Shottky	$\text{Ca}_A^X + B_B^X + 3\text{O}_O^X \rightarrow V_A^{''} + V_B^{''''} + 3V_O^{''''} + \text{CaBO}_3$	4.53	3.55	4.02	2.22
A , Shottky	$\text{Ca}_A^X + \text{O}_O^X \rightarrow V_A^{''} + V_O^{''''} + \text{CaO}$	4.11	3.42	3.50	1.26
B , Shottky	$B_B^X + 2\text{O}_O^X \rightarrow V_B^{''''} + 2V_O^{''''} + \text{BO}_2$	5.17	3.98	4.52	3.09

Energy of formation of the point defects (eV/defect)

Defect notation		CaSnO_3	CaTiO_3	CaZrO_3
Ca, vacancy	$V_A^{''}$	23.31	22.60	22.94
B , vacancy	$V_B^{''''}$	84.14	85.56	81.82
O1, vacancy	$V_{O1}^{''''}$	20.94	20.26	20.07
O2, vacancy	$V_{O2}^{''''}$	20.98	20.39	20.47
Ca, interstitial	$\text{Ca}_i^{''''}$	-13.64	-12.63	-14.86
B , interstitial	$B_i^{''''''}$	-61.52	-59.51	-57.12
O, interstitial	$O_i^{''''}$	-12.31	-11.58	-11.78

the overestimation of the bulk modulus of CaTiO_3 is much lower in [1], than in our calculation.

The calculated energies of intrinsic atomic defects indicate that Schottky-type defects are much more favorable than Frenkel-type defects in this type of crystals. This result is in agreement with previous calculations. The prediction of the enthalpies of mixing of the $\text{CaZr}_{1-x}\text{Ti}_x\text{O}_3$, $\text{CaZr}_{1-x} \times \text{Sn}_x\text{O}_3$ and $\text{CaSn}_{1-x}\text{Ti}_x\text{O}_3$ solid solutions fully correlates with the mismatch of sizes of substituting ions.

According to our calculation (Table 4 and Fig. 3), the lowest solution energies of the trivalent dopants correspond to cases of their incorporation on the B sites of the host crystal lattice and of their self-compensation by simultaneous incorporation on A - and B -sites. Thus, these processes are supposed to be the most energetically favorable. The most likely way of incorporation of the trivalent impurities on the Ca site is achieved by simultaneous substitution of another A^{2+} site by Na^+ ion. Such compensation mechanism occurs widely in natural processes. The compensation of an excess positive charge on the A -site by formation of $V_B^{''''}$ and $V_A^{''}$ vacancies is not so favorable. As seen from Table 4 and Fig. 3, the solution energies

are closely correlated with the size mismatch between a dopant ion and the host Ca^{2+} or B^{4+} ions.

The most favorable way of incorporation of the tetravalent ions M^{4+} is an isovalent substitution of B^{4+} ion. Their incorporation into the A positions accomplished by charge compensation with $V_B^{''''}$ and $V_A^{''}$ vacancies is much less preferable. According to our calculations, the solution energies of $M \rightarrow B$ substitutions are in direct relation with the size mismatch of the corresponding ions. However, the energies of Ca substitution by M^{4+} have a negative relation with their radii values. As can be seen from Fig. 3, the dependencies of $E(\delta^2)$ for the isovalent $M^{4+} \rightarrow B^{4+}$ substitutions do not come to 0 at $\delta = 0$, but the value of $E(\delta = 0)$ equals approximately from -0.5 to -1.0 eV. The latter is likely an estimate of an energy expense at the transition of fluorite-type oxides HfO_2 , UO_2 and ThO_2 with 8-fold coordination to 6-fold coordination in the final perovskite structure. Challenging future tasks of our investigations are attempts 1) to estimate dopant concentrations in dependence on the charge compensation way, 2) to calculate pair associates and more complicated clusters formation, 3) to predict temperature and pressure phase transitions, etc.

LITERATURE

1. Bassoli M., Buscaglia M.T., Bottino C. et al. Defect chemistry and dielectric properties of $\text{Yb}^{3+} : \text{CaTiO}_3$ perovskite // J. Appl. Phys. — 2008. — **103**, No 1. — P. 014104—014114.
2. Buckingham R.A. The Classical Equation of State of Gaseous Helium, Neon and Argon // Proc. Roy. Soc. London A. — 1938. — **168**, No 933. — P. 264—283.
3. Buttner R.H., Maslen E.N. Electron difference density and structural parameters in CaTiO_3 // Acta Crystallogr. C. — 1992. — **48**, No 5. — P. 644—649.

4. Davies R.A., Islam M.S., Gale J.D. Dopant and Proton Incorporation in Perovskite-Type Zirconates // *Sol. St. Ionics.* — 1999. — **126**, No 4. — P. 323—335.
5. Davies R.A., Islam M.S., Chadwick A.V., Rush G.E. Cation Dopant Sites in the CaZrO_3 Proton Conductor : A Combined EXAFS and Computer Simulation Study // *Ibid.* — 2000. — **130**, No 2. — P. 115—122.
6. Dick G.B., Overhauser A.W. Theory of the Dielectric Constants of Alkali Halide Crystals // *Phys. Rev.* — 1958. — **112**, No 1. — P. 90—103.
7. Gale J.D., Rohl A.L. The general lattice utility program (GULP) // *Mol. Simul.* — 2003. — **29**, No 5. — P. 291—341.
8. Galuskin E.V., Gazeev V.M., Armbruster Th. et al. Lakkargiite CaZrO_3 — a new mineral of the perovskite group from the North Caucasus, Kabardino-Balkaria, Russia // *Amer. Miner.* — 2008. — **93**, No 12. — P. 1903—1910.
9. Khan M.S., Islam M.S., Bates D.R. Cation Doping and Oxygen Diffusion in Zirconia : A Combined Atomistic Simulation and Molecular Dynamics Study // *J. Mater. Chem.* — 1998. — **8**, No 10. — P. 2299—2307.
10. Koopmans H.J.A., van de Velde G.M.H., Gellings P.J. Powder neutron diffraction study of the perovskites CaTiO_3 and CaZrO_3 // *Acta Crystallogr. C.* — 1983. — **39**, No 10. — P. 1323—1325.
11. Krayzman V., Levin I., Woicik J.C. et al. Effects of local atomic order on the pre-edge structure in the Ti K x-ray absorption spectra of perovskite $\text{CaTi}_{1-x}\text{Zr}_x\text{O}_3$ // *Phys. Rev. B.* — 2006. — **74**, No 22. — P. 224104—224131.
12. Kröger F.A., Vink H.J. Relations between concentrations of imperfections in crystalline solids // *Solid State Physics* / Ed. F. Seitz, D. Turnbull. — New York : Acad. Press, 1956. — Vol. 3. — P. 307—435.
13. Leonenko E.V. Atomistic computer modeling of TiO_2 — SnO_2 solid solutions : Master's thesis. — Moscow : Moscow State Univ., 2008. — 73 p.
14. Levin I., Cockayne E., Lufaso M.W. et al. Local Structures and Raman Spectra in the $\text{Ca}(\text{Zr}, \text{Ti})\text{O}_3$ Perovskite Solid Solutions // *Chem. Mater.* — 2006. — **18**, No 3. — P. 854—860.
15. Lewis G.V., Catlow C.R.A. Potential models for ionic oxides // *J. Phys. C.* — 1985. — **18**, No 6. — P. 1149—1161.
16. Lide D.R. The CRC Handbook of Chemistry and Physics, 73rd special student edition. — Boca Raton : CRC Press, 1994. — 2472 p.
17. Mather G.C., Islam M.S., Figueiredo F.M. Atomistic study of a CaTiO_3 -based mixed conductor : Defects, nanoscale clusters, and oxide-ion migration // *Adv. Func. Mater.* — 2007. — **17**, No 6. — P. 905—912.
18. Minervini L., Grimes R.W., Sickafus K.E. Disorder in Pyrochlore Oxides // *J. Amer. Ceram. Soc.* — 2000. — **83**, No 8. — P. 1873—1878.
19. Mott N.F., Littleton M.J. Conduction in polar crystals. I. Electrolytic conduction in solid salts // *Trans. Faraday Soc.* — 1938. — **34**. — P. 485—499.
20. Ross N.L., Angel R.J., Kung J., Chaplin T.D. Elastic Properties of Ca-perovskites // *Mat. Res. Soc. Symp. Proc.* — 2002. — **718**. — P. 115—119.
21. Shannon R.D. Revised effective ionic radii and systematic studies of interatomic distances in halides and chalcogenides // *Acta Crystallogr.* — 1976. — **32**, No 2. — P. 751—767.
22. Urusov V.S. Crystal chemical and energetic characterization of solid solution // *Adv. Phys. Geochem.* — 1992. — **10**, No 6. — P. 162—193.
23. Urusov V.S. Comparison of semi-empirical and ab-initio calculations of the mixing properties of MO-M' O solid solutions // *J. Solid State Chem.* — 2000. — **153**, No 2. — P. 357—364.
24. Urusov V.S. The phenomenological theory of solid solutions // *Solid solutions in silicate and oxide systems. EMU Notes in Mineralogy.* — Budapest : Eotvos Univ., 2001. — **3**. — P. 121—153.
25. Vegas A., Vallet-Reg M., Gonzales-Calbet J.M., Alario-Franco M.A. The ASnO_3 ($A = \text{Ca}, \text{Sr}$) perovskites // *Acta Crystallogr. B.* — 1986. — **42**, No 2. — P. 167—172.
26. Woodward P.M. Octahedral Tilting in Perovskites. I. Geometrical Considerations II. Structure Stabilizing Forces // *Ibid.* — 1997. — **53**, No 1. — P. 44—66.
27. Yashima M., Ali R. Structural Phase Transition and Octahedral Tilting in the Calcium Tinanate Perovskite CaTiO_3 // *Sol. St. Ionics.* — 2009. — **180**, No 1. — P. 120—126.
28. Zelezny V., Limonov M.F., Usvyat D. et al. Soft-mode behavior of incipient ferroelectric perovskite CaTiO_3 // *Ferroelectrics.* — 2002. — **272**, No 1. — P. 113—118.

Received 12.01.2012

*B.C. Урусов, Е.В. Леоненко*АТОМИСТИЧЕСКОЕ КОМПЬЮТЕРНОЕ МОДЕЛИРОВАНИЕ ПЕРОВСКИТОВ ABO_3 ($A = \text{Ca}; B = \text{Zr}, \text{Ti}, \text{Sn}$): КРИСТАЛЛИЧЕСКАЯ СТРУКТУРА, СОБСТВЕННЫЕ ДЕФЕКТЫ И ОБРАЗОВАНИЕ ПРИМЕСЕЙ

Проведено моделирование структурных и термодинамических свойств сложных оксидов с ромбической перовскитовой структурой CaZrO_3 , CaTiO_3 и CaSnO_3 . Для расчетов использовали метод атомистических парных потенциалов в ионном приближении. Результаты моделирования структурных свойств хорошо согласуются с экспериментальными данными и предыдущими вычислениями, в то время как вычисленные значения модулей упругости завышены относительно экспериментальных. Вычисленные значения энтропии для комнатной температуры хорошо согласуются с экспериментальными данными для CaTiO_3 и CaZrO_3 . Впервые для этих трех оксидов проведены расчеты энтропии в температурном диапазоне 300—1800 К. Результаты согласуются с экспериментальными данными для CaTiO_3 . С помощью метода Мотта-Литтлтона вычислены значения энергии образования изолированных собственных точечных дефектов в этих кристаллах. Для всех трех перовскитовых структур наиболее энергетически выгодным является Ca—O дефект Шоттки. Значения энергии смешения при изовалентном вхождении четырехвалентных ионов ($\text{Zr}^{4+}, \text{Ti}^{4+}, \text{Sn}^{4+}, \text{Hf}^{4+}, \text{U}^{4+}, \text{Th}^{4+}$) в CaZrO_3 , CaTiO_3 ,

$CaSnO_3$ получены в приближении бесконечного разбавления. На основе этих данных были вычислены значения энталпии смешения протяженных бинарных твердых растворов $CaZrO_3$ — $CaTiO_3$, $CaTiO_3$ — $CaSnO_3$, $CaSnO_3$ — $CaZrO_3$. Проведено моделирование вхождения изолированных трехвалентных (Sc^{3+} , Y^{3+} , Cr^{3+} , Fe^{3+} , La^{3+}) и четырехвалентных (Hf^{4+} , U^{4+} , Th^{4+}) примесей в позиции A и B ($A = Ca, B = Zr, Ti, Sn$) для всех трех перовскитов. Согласно расчетам, наиболее энергетически выгодным механизмом вхождения трехвалентных примесей M^{3+} является одновременное замещение ионов в позициях A и B перовскитовой структуры. Наиболее выгодный путь вхождения четырехвалентных ионов M^{4+} — изовалентное замещение иона B^{4+} .

B.C. Урусов, Є.В. Леоненко

**АТОМІСТИЧНЕ КОМП'ЮТЕРНЕ
МОДЕЛЮВАННЯ ПЕРОВСЬКІТІВ ABO_3
($A = Ca; B = Zr, Ti, Sn$): КРИСТАЛІЧНА
СТРУКТУРА, ВЛАСНІ ДЕФЕКТИ
І УТВОРЕННЯ ДОМІШОК**

Проведено моделювання структурних і термодинамічних властивостей складних оксидів з ромбічною перовськітовою структурою $CaZrO_3$, $CaTiO_3$ і $CaSnO_3$. Для розрахунків використовували метод атомістичних парних потенціалів у іонному наближенні. Результати моделювання структурних властивостей доб-

ре узгоджуються з експериментальними даними і попередніми обчисленнями, тоді як обчисленні значення модулів пружності завищені щодо експериментальних. Обчисленні значення ентропії для кімнатної температури добре узгоджуються з експериментальними даними для $CaTiO_3$ і $CaZrO_3$. Вперше для цих трьох оксидів проведенні розрахунки ентропії в температурному діапазоні 300—1800 К. Результати узгоджуються з експериментальними даними для $CaTiO_3$. За допомогою методу Мотта-Літтлтона були обчислені значення енергії утворення ізольованих власних точкових дефектів в цих кристалах. Для всіх трьох перовськітів структур найбільш енергетично вигідним є $Ca-O$ дефект Шоттки. Значення енергії зміщення за ізовалентного вхождження чотиривалентних іонів (Zr^{4+} , Ti^{4+} , Sn^{4+} , Hf^{4+} , U^{4+} , Th^{4+}) у $CaZrO_3$, $CaTiO_3$, $CaSnO_3$ отримані в наближенні несікінченного розбавлення. На основі цих даних були обчислені значення енталпії зміщення протяжних бінарних твердих розчинів $CaZrO_3$ — $CaTiO_3$, $CaTiO_3$ — $CaSnO_3$, $CaSnO_3$ — $CaZrO_3$. Проведено моделювання вхождения ізольованих тривалентних (Sc^{3+} , Y^{3+} , Cr^{3+} , Fe^{3+} , La^{3+}) і чотиривалентних (Hf^{4+} , U^{4+} , Th^{4+}) домішок в позиції A і B ($A = Ca, B = Zr, Ti, Sn$) для всіх трьох перовськітів. Згідно розрахункам, найбільш енергетично вигідним механізмом вхождения тривалентних домішок M^{3+} є одночасне заміщення іонів в позиціях A і B перовськітової структури. Найвигідніший шлях вхождения чотиривалентних іонів M^{4+} — ізовалентне заміщення іона B^{4+} .